The Three-Dimensional Facies Architecture of Terrigenous Clastic Sediments and Its Implications for Hydrocarbon Discovery and Recovery (CSP3), 1992

THE LARGE-SCALE ARCHITECTURE OF THE FLUVIAL WESTWATER CANYON MEMBER, MORRISON FORMATION (UPPER JURASSIC), SAN JUAN BASIN, NEW MEXICO

E. JUN COWAN
Department of Geology,
University of Toronto,
Toronto, Ontario, Canada M5S 3B1

ABSTRACT: The Westwater Canyon Member of the Morrison Formation (Upper Jurassic) has previously been interpreted as consisting of fluvial "channel systems" tens of kilometers wide and tens of meters thick. Reinvestigation of the member indicates that these "channel systems" actually represent post-depositional aquifer conduits, defined instead by differing sandstone colors, rather than primary depositional features. The member is composed of amalgamated, individual fining-up sandstone sheets each about 5-10 m thick. The absolute widths of these sheet sandstone bodies are at least 1 km and possibly exceed several kilometers. The width:thickness range of the sandstone sheets are well within the typical values of sandstone body dimensions reported from other fluvial sandstones, and are interpreted to represent aggradational channel-belts. Sandstone bodies thicker than about 12 m are the result of amalgamation of these individual unit sandstone bodies, and do not represent individual channel belts as interpreted previously.

Internally, the sheets contain abundant concave-up troughs typically 30 m wide and 5 m thick, filled both laterally and vertically with inclined parallel- to low-angle cross-stratified sandstone, in places exhibiting parting lineation. The laterally-limited extent of these large troughs and nature of their internal fills suggest that they represent short-lived scour fills rather than confined elongated channels. The concave-up erosional base, a negative feature, was most likely formed due to large-scale flow separation within a wider and shallower channel. Physical conditions similar to stream-flow convergence at channel confluences may be responsible for their formation. The abundant preservation of these troughs in the Westwater Canyon Member is consistent with the expected poor preservation of positive barforms in a sweeping, sandy-braided channel belt.

Review of the literature indicates that inferred channelbelt sandstone bodies mostly fall within the thickness range of 1 to 12 m, irrespective of their interpreted fluvial style. Post-depositional large-scale reservoir conduits are also expected to fall within this range for sandy fluvial systems. Deviations from this range are due to amalgamation of the sandstone bodies or increased grain-size heterogeneity, resulting in an increase and decrease, respectively, of the conduit size.

INTRODUCTION

Clarifying the origin and post-depositional burial history of fluvial-sandstone bodies is critical to understanding the scale and role of heterogeneities involved in the migration of pore fluids following the burial of sandy fluvial deposits (cf. Miall, 1988b). The architecture of sandstone bodies resulting from channelbelt avulsion and coeval basinal subsidence has been modeled quantitatively by several workers (Alexander and Leeder, 1987; Allen, 1978, Bridge and Leeder, 1979; Leeder, 1978). These quantitative models are able to predict depositional patterns resulting from syndepositional subsidence and repeated avulsion of channel belts. The resulting architecture of the sandstones controls the pore-fluid flow, and hence influences hydrocarbon migration and the emplacement of some economic metalliferous ores, such as uranium. Application of these models requires the field recognition of individual channelbelt deposits. There are, however, few field descriptions in the fluvial literature, especially those of sandy multichannel fluvial systems, which differentiate individual channel belts from laterally and vertically interconnected channelbelt deposits.

One of the best-known examples of the documentation of alluvial architecture is that of Campbell (1976) on the Upper Jurassic Westwater Canyon Member of the Morrison Formation, San Juan Basin, New Mexico. Campbell's work has been extensively cited as a typical example of a braided river deposit involving the preservation of laterally coalesced "channel systems" and "smaller channels" and has been repeatedly used in textbooks (e.g., Cant, 1978; Leeder, 1982; Collinson, 1986). These "channel systems" were described by Campbell (1976) to be vertically and laterally coalesced, and to range in width from 1.6 to 34 km and in thickness from 6 to 61 m. Individual "smaller channels" have widths of 30 to 366 m and depths from 1 to 6 m (Campbell, 1976).

On the basis of detailed outcrop studies, this paper shows that the "channel systems" of Campbell (1976) do not represent depositional channels, but are post-depositional aquifer conduits or permeability-pathway compartments. The conduits (identified on the basis of color, which reflect the state of sandstone oxidation) are up to several tens of meters thick, and were formed by the vertical coalescence of sandstone sheets about 5-10 m in thickness, interpreted here to represent channelbelt deposits. The sheets are internally composed of large concave-up features ("smaller channels" of Campbell, 1976) which are interpreted to represent large scour fills produced in a wide braided channel belt.

GEOLOGICAL OVERVIEW

The Upper Jurassic Morrison Formation was deposited in the San Juan Basin (Figs. 1a, b) which lay several hundred kilometers east of a Late Jurassic Andean-type, magmatic arc. The detrital infill is derived from the uplifted edge of the foreland (cf. Turner-Peterson and Fishman, 1986). The Morrison Formation (mean thickness 200 m), famous for hosting more than half the uranium reserves in the United States, is divided into three members in the study area (Fig. 2), which are in ascending order 1. Recapture Member, a lithologically heterogeneous unit comprising interfingering fluvial, lacustrine and eolian deposits; 2. the Westwater Canyon Member, a laterally extensive fluvial sandstone; and 3. the Brushy Basin Member, a playa lake complex (Turner-Peterson, 1985, 1986; Turner-Peterson and Fishman, 1988). The Westwater Canyon Member underlies and interfingers with the overlying Brushy Basin Member along an arbitrary boundary. The Brushy Basin Member was truncated by late Early Cretaceous erosion during uplift along the southern margin of the San Juan Basin. In the southwestern portion of the basin, the Upper Cretaceous Dakota Sandstone directly overlies the Westwater Canyon Member, whereas toward the east the Brushy Basin Member thickens at the expense of the Westwater Canyon Member.

Clear breaks in the stratigraphy, together with differing pebble lithologies, were used by Turner-Peterson (1986) to divide the Westwater Canyon fluvial unit into three submembers thought to represent separate fluvial episodes. On the basis of trough cross-stratification orientations, Turner-Peterson (1986) concluded that the lower fluvial unit shows a northeast to east-northeasterly-directed, basin-wide paleoflow pattern, whereas the middle and upper units showed a basin-wide southeast to east-southeasterly-directed pattern. The overlying Poison Canyon Sandstone (a unit belonging to the Brushy Basin Member of the eastern San Juan Basin) and its possible equivalents showed a return to a northeasterly-directed paleoflow. These patterns are quite different from the paleoflow pattern of Campbell (1976), who considered the whole of the member to have been deposited by a northeasterly-directed fluvial system. The paleoflow directions of Turner-Peterson (1986) show that Campbell's (1976) transect of the fluvial system is subparallel to the regional paleoslope and is not transverse, as Campbell (1976) suggested. Consequently, transverse views of the Westwater fluvial system, as illustrated by Campbell (1976, his Fig. 2, and Fig. 3 herein), are unlikely to represent channel cross sections.

Miall and Turner-Peterson (1989) re-studied the Westwater Canyon Member utilizing the conceptual six-fold hierarchial subdivision of bounding surfaces (Miall, 1988c). Individual lithofacies (cf. Miall, 1978) were identified and separated, then combined into lithofacies assemblages defining "architectural elements" (cf. Miall, 1985). The presence of lateral-accretion deposits along with downstream-accreted macroforms in the same exposures, was interpreted to be the product of sandflat deposition in a low-sinuosity, multiple-channel river. They could not find support for the fining-upward channel-fill cycles as documented by Campbell (1976). The present study supports the braided channel interpretation of Miall and Turner-Peterson (1989), but many of the structures interpreted to represent lateral/downstream-accretion macroforms are reinterpreted herein as laterally restricted scour fills formed in a wide braided-channel belt. Fining-upward cycles in this unit have now been documented by Godin (1991).

The purpose of this paper is to describe the architecture of the Westwater Canyon Member at two scales. 1. The first deals with the structures at the member scale and describes the largest architectural component of the Westwater Canyon Member, namely ~5- 10-m-thick sandstone sheets. The identified sheets are contrasted with Campbell's (1976) architectural reconstruction of the member. 2. The second scale of description details the internal architecture of the sheet sandstones identified in part one, as well the significance of abundant large troughs (typically 30 x 5 m) present in the sheets.

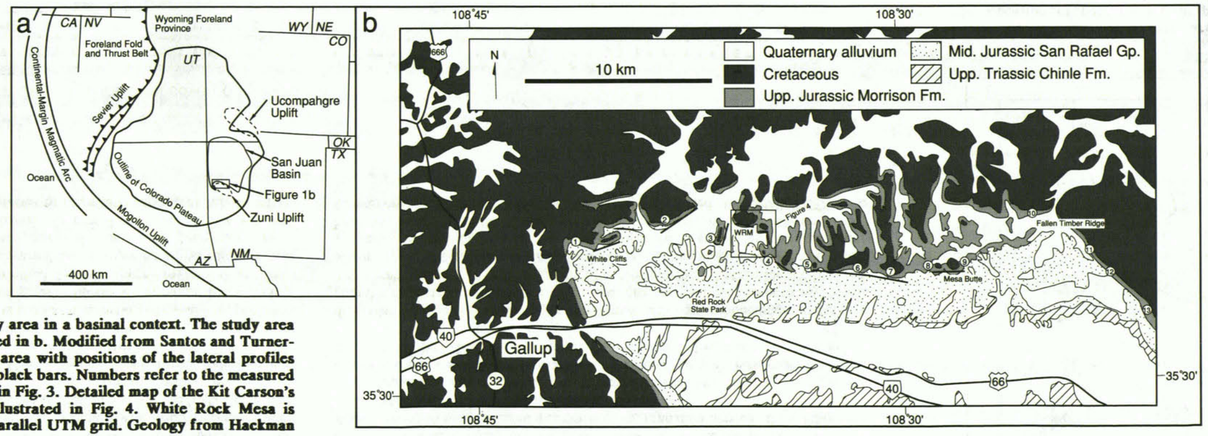

FIG. 1.—a. Location of the study area in a basinal context. The study area enclosed in the rectangle is detailed in b. Modified from Santos and Turner-Peterson (1986, Fig. 3). b. Study area with positions of the lateral profiles used to construct Fig. 6 shown as black bars. Numbers refer to the measured sections of Campbell, also shown in Fig. 3. Detailed map of the Kit Carson's Cave area, shown enclosed, is illustrated in Fig. 4. White Rock Mesa is labeled as 'WRM'. Map borders parallel UTM grid. Geology from Hackman and Olson (1977).

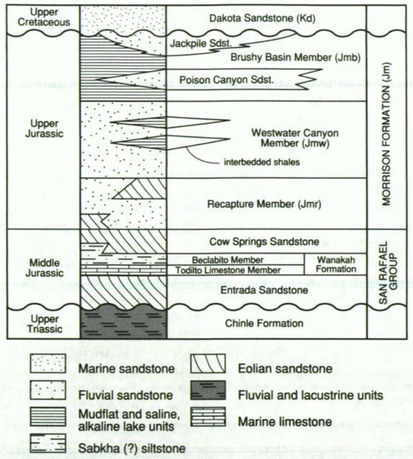

Fig. 2.—Generalized stratigraphy of the Jurassic strata, as exposed in the uplifted edge of the southern San Juan Basin. From Turner-Peterson (1986, Fig. 2)

METHODS

The Westwater Canyon Member crops out discontinuously for about 500 km around the west and southern uplifted margins of the San Juan Basin. Photomosaics were produced from oblique aerial and ground photographs along a transect on the east-west-trending cliff forming the southern margin of the basin, exposed in northwest New Mexico (Fig. 1b). These were used as base maps for plotting major surface traces of the lithologic boundaries, both with the aid of binoculars and by walking the outcrop where possible. Four profiles in the Kit Carson's Cave area were examined where the exposure was flat enough to permit inspection on a more detailed level (Fig. 4).

The outcrop shown in Figure 5 illustrates the nature of the Westwater Canyon Member at White Cliffs. The original drawings of similar cliff exposures were redrawn at a vertical exaggeration of five, and each of these profiles was projected into the plane joining Campbell's (1976, his Fig. 2) measured sections 1 and 9 (see Fig. 1b). Campbell's profile (Fig. 3) was also redrawn to match the x5 vertical exaggeration of the profile presented here to enable direct visual comparison (Fig. 6). Sandstone color was noted and divided into three broad categories; white, buff and red.

The descriptive terminology of sandstone bodies used here follows that of Friend and others (1979) who introduced a classification scheme based on the width:thickness ratio of sandstone bodies. Sandstones with width:thickness ratios less than 15:1 are termed ribbon-sandstone bodies, and sandstone bodies that have width:thickness ratios of over 15:1 are termed sheet-sandstone bodies. The sandstone bodies of the Westwater Canyon Member all display ratios greatly exceeding 15 and are therefore identified as sheet sandstones.

The lithofacies scheme follows that of Miall (1978) with modifications (Table 1). Lithofacies within the sandstone sheets include horizontal and parallel upper-flow-regime stratification (Sh), inclined and parallel upper- to transitional-flow-regime stratification (Si), low-angle cross-stratified (<10°) upper- to transitional-flow-regime stratification (Sl), trough cross-stratification represents lower-flow-regime three-dimensional dunes (St), topset-preserved convex-up humpback cross-stratification (Sthb) and rare climbing ripple cross-lamination (Sr), which was identified at only one location. Lithofacies Si essentially represents lithofacies Sh that formed on an inclined surface (see Paola and others, 1989, their Fig. 2). By far the most predominant lithofacies are Si, Sl and Sh which make up more than 80% of the deposit and were difficult to separate because of complex gradations. Another lithofacies, Sthb, although subordinate in occurrence, is interpreted to be the product of deposition from humpback dunes (cf. Saunderson and Lockett, 1983; Allen, 1983a). A more detailed discussion of the gradation between these lithofacies is presented in Cowan (1990) and Godin (1991).

The bounding-surface subdivision employed in the detailed profiles of the Kit Carson's Cave area (Fig. 4) is modified from Miall (1988c). First-order bounding surfaces that bound sets of lithofacies are not illustrated here in all profiles unless indicated. Second-order bounding surfaces are planes that separate cosets of dissimilar lithofacies. In this paper third- and fifth -order bounding surfaces are laterally restricted and extensive, discordant erosional surfaces respectively. Sixth-order bounding surfaces are essentially fifth-order surfaces, but are located between major depositional systems (such as formational boundaries). Third-order bounding surfaces are commonly concave-up in sectional view, and fifth- and sixth-order bounding surfaces are flat across most of the exposures, but may undulate locally. Convex-up fourth-order bounding surfaces, interpreted by Miall (1988c) to represent constructional surfaces of macroforms, were not recognized in the study.

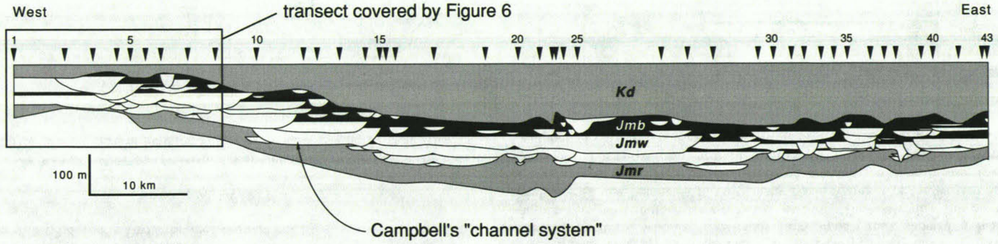

Fig. 3.—Cross section of the Morrison Formation according to Campbell (1976, his Fig. 2). The rectangle represents the re-examined section as presented in this study (Fig. 1b), and illustrated in Fig. 6. Stratigraphic abbreviations are: Recapture Member of the Morrison Formation (Jmr), Westwater Canyon Member (Jmw), Brushy Basin Member (Jmb), Dakota Sandstone (Kd). Numbers refer to the measured sections of Campbell (1976). Vertical exaggeration is x52. The upper surface of Kd is not the actual top of the Dakota Sandstone.

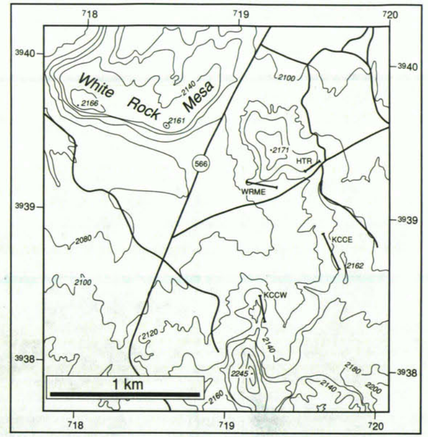

Fig. 4.—The Kit Carson's Cave area in detail. Contours in 20-m intervals. Location of detailed lateral profiles (Figs. 7, 10, 13 and 16) labeled: White Rock Mesa East (WRME), Hill Top Road (HTR), Kit Carson's Cave East (KCCE), Kit Carson's Cave West (KCCW). 1-km² UTM grid reference from Church Rock 24,000 topographic sheet.

PART I: THE LARGE-SCALE SANDSTONE SHEETS OF THE WESTWATER CANYON MEMBER

Of the large-scale profiles, only the White Cliffs profile located on the westernmost end of Campbell's (1976) profile (Fig. 3), is described in detail here. Other profiles are simplified and presented as Figure 6.

White Cliffs Profile

At White Cliffs (Fig. 5) the lower basal contact of the Westwater Canyon Member with the underlying Recapture Member is sharp, and can be followed consistently across the exposure. The sixth-order erosional bounding surface between the Westwater Canyon Member and the overlying Dakota Sandstone is also sharp, but attains a relief of several meters just east of the break in the cliff line (Fig. 5). The overlying Dakota Sandstone is a black carbonaceous shale, a

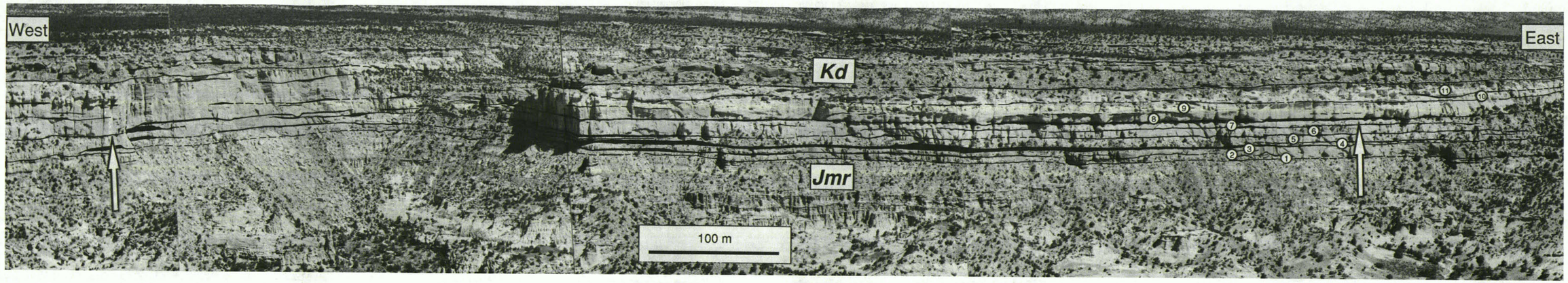

FIG. 5.—An example of a cliff profile from White Cliffs (refer to Fig. 1b for location). Each sheet-sandstone body composing the member is numbered one to eleven on the eastern end of the profile. Note the amalgamating nature of the sandstone sheets toward the western end of the profile. Vertical sandstone color changes (marked by arrows - see text for explanation) are controlled by the preservation of thick overbank deposits, shown in black.

yellowish sandstone, or interbeds of these two lithologies.

The Westwater Canyon Member at White Cliffs is composed of eleven vertically stacked sandstone sheets, as defined on the eastern portion of the profile; due to extensive amalgamation, the units are not readily seen on the western side. The sheets have flat, erosive bases, except for isolated concave-up erosional bases, which are several tens of meters wide, and display reliefs of 2 to 5 m (Fig. 5). The sheets are ~5 m thick and are capped by green/red/white-colored fine sandstone and subordinate shales which are interpreted to be of fluvial overbank affinity. The basic building blocks of the member are these sandstone-overbank couplet sheets. At White Cliffs, the paleocurrents from trough cross-stratified sets indicate a largely easterly directed paleoflow, that is, to the right and obliquely out of the profile, which trends 252° to 072° (Fig. 5). Sheets are inferred to be tabular in three dimensions, but locally show marked lateral thinning on the scale of the exposure. Sandstone sheet 5, for example, can be followed from east to west where it bifurcates and becomes interlayered with overbank deposits of the same order of thickness as the sandstone body, indicating proximity to an edge of the sheet. Therefore, the edges of these tabular sandstone sheets are inferred to have a very low-angle wedge shape. In most of the other studied exposures, however, the lateral terminations of the sandstone sheets are not commonly observable, most likely because the cliff faces are orientated subparallel to the easterly directed paleoflow, and as a result, subparallel to the long axes of the sheet sandstones as well.

The overbank deposits can reach thicknesses of up to 3 m at White Cliffs (as can be seen in the center of the profile; Fig. 5), but commonly are thinner, truncated in many places by the overlying sandstone sheet. The lateral variation in color of the sandstone is evident from this exposure (the color boundaries are schematically represented in Fig. 6). The boundary between white- and buff-colored sandstone is located a third of the height up from the base of the Westwater Canyon Member on the western side of the profile, whereas a similar color boundary is located higher up to the east. At both ends of the profile, the vertical color change corresponds to horizons with marked preservation of overbank deposits (at arrows shown in Fig. 5).

Composite Lateral Profiles

The lateral extent of the profiles presented in Figure 6 starts at the westernmost portion of Campbell's (1976) transect and follows through to his measured section 9 (Figs. 1b, 3), which represents one fifth of the transect of Campbell (1976).

Individual erosional bounding surfaces are difficult to trace entirely along more than 1.5 km of cliff line (Fig. 6). The erosion surfaces are lost where the sandstone sheets amalgamate. Amalgamated erosional surfaces can be identified by intraclast horizons within the amalgamated unit, but in many cases these horizons are missing. It should be noted that, in general, it is not possible to trace the base of a sandstone sheet across to adjacent cliff exposures separated by valleys. This is contrary to the documentation of Campbell (1976), in which his westward overstepping pattern of the "channel systems" in the Westwater Canyon Member (Fig. 3) is entirely based on the ability to trace these bounding surfaces laterally for long distances.

The color of the sandstone is highly variable from one cliff exposure to another; however, white alteration is always underlain by reddish-colored sandstone, never the reverse. The boundaries of these color changes are laterally gradational but are vertically abrupt at any one location. They commonly coincide with bases of sheet sandstones where the erosion surface has not truncated the underlying overbank deposit (White Cliffs and White Rock Mesa areas, Fig. 6). White sandstones in places occur completely enclosed in fine-grained overbank deposits in the eastern sections (i.e. in two dimensions, e.g., Mesa Butte, Fig. 6). The lateral variation in color change does not coincide with obvious lateral terminations of the sheet sandstones.

Interpretation of the large-scale profiles

The inspection of the sandstone color distribution in the Westwater Canyon Member, as summarized in Figure 6, indicates that the vertical amalgamation of the fluviatile sheet sandstones played an important role in controlling the final sandstone color distribution within the Westwater Canyon Member. The origin of

TABLE 1.—The main lithofacies of the Westwater Canyon Member, based partly on Miall's (1978) lithofacies codes.

LITHO-FACIES CODE	GRAIN SIZE	CHARACTER AND STRATIFICATION	INTERPRETATION	OCCURR-ENCE
Sh	v. fine to very coarse sand	parting lineation, subhorizontal stratification; closely associated and gradational with Si / Sl	upper flow regime plane bedding by suspension fall out, low relief bed forms	common
Si/Sl	v. fine to v. coarse sand	sporadic parting lineation; inclined parallel stratification (Si), or less than 10 degrees angular discordance (Sl) to the underlying bounding surface; in places appear broad trough shape	upper to transitional flow regime structure, see Paola et al. (1989)	very common
St	med to v. c. sand, may be pebbly	0.2 - 0.6 m thick sets; commonly occur as cosets; interstratified wih Si/Sl, Sh; coarser grained than Si/Sl or Sh	lower flow regime 3D dunes	fairly common
Sthb	v. f. to v. c. sand, may be pebbly	fine subhorizontal topsets grade into coarser grained, sometimes pebbly foresets; appear trough shaped in transverse section and convex-up (humpback - hb) in longitudinal section	transitonal flow regime humpback dunes or bar forms; see Allen (1983a), Saunderson & Lockett (1983)	subordinate
Sr	very fine sandstone	occur as A or B type climbing ripple cross lamination	lower flow regime 3D ripples	rare

Continued on page 84

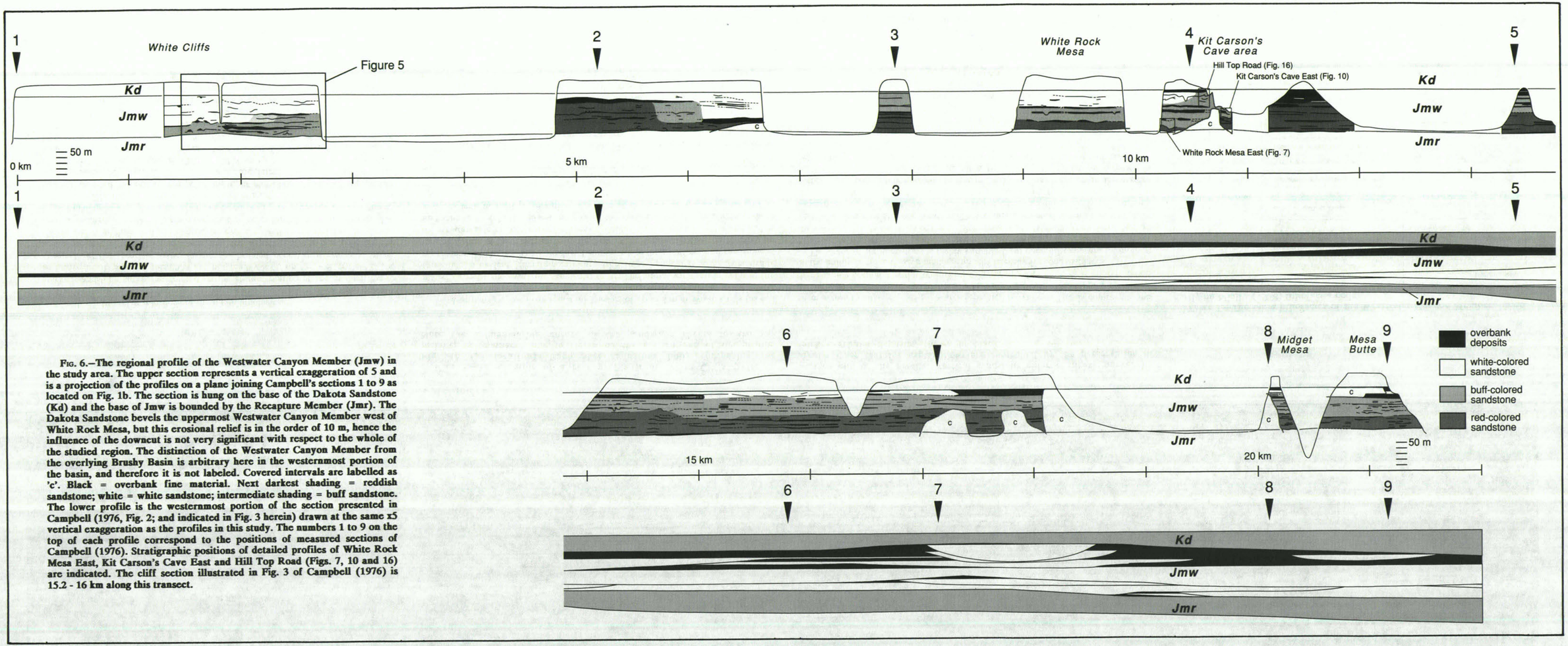

FIG. 6.—The regional profile of the Westwater Canyon Member (Jmw) in the study area. The upper section represents a vertical exaggeration of 5 and is a projection of the profiles on a plane joining Campbell's sections 1 to 9 as located on Fig. 1b. The section is hung on the base of the Dakota Sandstone (Kd) and the base of Jmw is bounded by the Recapture Member (Jmr). The Dakota Sandstone bevels the uppermost Westwater Canyon Member west of White Rock Mesa, but this erosional relief is in the order of 10 m, hence the influence of the downcut is not very significant with respect to the whole of the studied region. The distinction of the Westwater Canyon Member from the overlying Brushy Basin is arbitrary here in the westernmost portion of the basin, and therefore it is not labeled. Covered intervals are labelled as 'c'. Black = overbank fine material. Next darkest shading = reddish sandstone; white = white sandstone; intermediate shading = buff sandstone. The lower profile is the westernmost portion of the section presented in Campbell (1976, Fig. 2; and indicated in Fig. 3 herein) drawn at the same x5 vertical exaggeration as the profiles in this study. The numbers 1 to 9 on the top of each profile correspond to the positions of measured sections of Campbell (1976). Stratigraphic positions of detailed profiles of White Rock Mesa East, Kit Carson's Cave East and Hill Top Road (Figs. 7, 10 and 16) are indicated. The cliff section illustrated in Fig. 3 of Campbell (1976) is 15.2 - 16 km along this transect.

the various shades of sandstone colors, and their vertical and lateral distributions, can only be understood by examining the diagenetic history of the Westwater Canyon Member, as discussed below.

Diagenetic history of the Westwater Canyon Member. The sandstone colors observable in the cliff exposures of the Westwater Canyon Member are the cumulative result of three known diagenetic events that occurred during the Jurassic to Tertiary Periods (see Turner-Peterson, 1985, 1986; Granger and Santos, 1986; Hansley, 1986). Two episodes of bleaching, resulting in either the reduction or removal of iron from the detrital grains, left some Westwater Canyon Member sandstones either gray or white. The first episode occurred in the Late Jurassic to Early Cretaceous and was related to alkaline, organic-rich fluids, and the second episode occurred in the Late Cretaceous, and was related to acid, organic-rich fluids. The prominent red color of the member represents the third, and most recent coloration, which is linked to a Tertiary oxidation event. These diagenetic events are summarized as follows.

1. The initial alteration, during the Late Jurassic to Early Cretaceous, was caused by organic acids expelled down from the fine-grained mudstone units in the overlying Brushy Basin Member, which reacted with iron-titanium oxides (chiefly magnetite and ilmenite) in the sandstones of the Westwater Canyon Member (Turner-Peterson, 1986). Iron leached from the detrital grains formed pyrite. More recent oxidation of pyrite (beginning in the Tertiary and continuing today) resulted in a yellowish-gray color in surface exposures of these sandstones. This first alteration event has been linked to the emplacement of primary tabular uranium ore in the Westwater Canyon Member (Granger and Santos, 1986).

2. Further localized removal and/or reduction of iron from the sandstones in the Westwater Canyon Member sandstone was the result of the downward percolation of acidic, organic-rich fluids from carbonaceous shales of the Dakota Sandstone during the Late Cretaceous. This was only possible in the southwestern portions of the basin after the pre-Dakota erosion of the lacustrine Brushy Basin Member and deposition of carbonaceous black shales of the Dakota Sandstone directly on permeable sandstones of the Westwater Canyon Member (Turner-Peterson, 1986). The acidic nature of the organic-rich fluids derived from the Dakota resulted in kaolinitization of feldspars (Turner-Peterson, 1986). Pronounced localized "bleaching" of the Westwater Canyon Member in the study area (e.g., White Rock Mesa) has been attributed by Turner-Peterson (1986) to this alteration event.

3. The red coloration of the sandstone is attributed by Granger and Santos (1986) to a subsequent oxidation event, which contributed to the formation of redistributed uranium ore within the member. This occurred because of an increase in hydrodynamic flow of oxidizing meteoric water from the uplifted southern edge of the San Juan Basin along the Zuni Uplift (Figs. 1a, b) during the Tertiary associated with the regional Laramide orogeny (Granger and Santos 1986). Sandstones that escaped earlier removal and/or reduction of iron in the previous reducing events were oxidized and now display a prominent red coloration. The intermediate buff-colored sandstones may have been partially leached of iron during the two earlier alteration events, so that these sandstones were not as readily reddened during the later Tertiary oxidation event (Turner-Peterson, 1986, pers. commun., 1990).

Reassessment of Campbell's architectural model. The ~5- to 10-m-thick sandstone sheets, irrespective of their color, are here recognized as the largest architectural component of the Westwater Canyon Member, whereas the thicker sandstones represent intervals of amalgamated sandstone sheets. It is apparent that the presence or absence of impermeable tabular overbank deposits exerted primary control on the migration of pore fluids through the Westwater Canyon Member during its burial history, and hence the subsequent color variation of the member (Figs. 5, 6).

Campbell (1976) identified two scales of channel-filling deposits. The largest, which he termed "channel systems", are shown in his constructed profile of the Westwater Canyon Member (reproduced in Fig. 3 herein). He described the "channel systems" to be:

> "...tabular in cross-section with abrupt edges only at the channel edges. Separate channel systems commonly are marked by contrasting overall colors on outcrops such as grayish-red versus salmon-pink versus buff" (Campbell, 1976, p. 1013).

According to Campbell's cross section, the abrupt "channel system" edges were mostly inferred and are shown as dashed lines (Campbell, 1976, his Fig. 2). The color differences in the sandstones were partly used in the definition of the "channel system" boundaries as defined by Campbell (1976). The White Cliffs section (Fig. 5), which coincides with Campbell's section 1, can be broadly divided into two units according to the sandstone color at any one vertical section. These color units can be clearly correlated to Campbell's section as representing "channel system" bodies (Figs. 3, 6). At the location of Campbell's measured section 3, the Westwater Canyon Member is divided into two "channel system" deposits, again corresponding to two distinct differences in sandstone color. It is evident that the uppermost "channel system," which is represented at Campbell's sections 2, 3 and 4, coincides with the white to buff sandstone color as documented in the upper profile of Figure 6 (6 to 10.6 km along transect). There is a complex of channel deposits figured in Campbell's cross section between Kit Carson's Cave area and Midget Mesa (sections 4 to 8), where the "channel system" boundaries were apparently established using a combination of the sandstone color and the presence of overbank material between the sandstone sheets. At section 9 (Fig. 6, 21.2 km along transect), however, the boundary follows the above-mentioned color change criterion, and the "channel system" boundaries clearly coincide with the color change seen in the exposure.

Lateral color changes were not observed to coincide with sandstone-sheet edges and do not represent depositional features, but they do seem to coincide in places with the geometry of Campbell's (1976) "channel systems". It can be concluded, therefore, that Campbell (1976) was partly identifying post-depositional aquifer conduits or permeability-pathway compartments as primary depositional features. Furthermore, his cross section cannot be used as a map of post-depositional aquifers, since some of his channel boundaries are not defined solely by the sandstone color change, and many of the channel boundaries correspond to areas of no outcrop (Fig. 6). It is evident that the depositional "channel systems" of Campbell (1976), in the order of tens of meters thick, do not exist; instead, the ~5- 10-m-thick sandstone sheets are here recognized as the principal architectural component of the Westwater Canyon Member.

PART II: INTERNAL ARCHITECTURE OF THE SANDSTONE SHEETS

The sandstone sheets, as described earlier, are internally composed of structures that were termed "smaller channels" by Campbell (1976). These structures, as well as large macroforms, are described and interpreted in this section.

Lateral Profiles of the Kit Carson's Cave Area

The Kit Carson's Cave area is located approximately 1 km southeast of White Rock Mesa, and 4 km north-northeast of Red Rock State Park (Figs 1b, 4). Three profiles, White Rock Mesa East, Kit Carson's Cave East and Kit Carson's Cave West, are stratigraphically located immediately above the Westwater and Recapture Member contact, and the Hill Top Road profile lies just below the Westwater Canyon Member-Dakota Sandstone contact (Fig. 1b). The strata are tilted approximately 4° to the north-northwest. However, since the tilt is not appreciable, and to avoid introducing error in the data processing, the individual azimuth data were not rotated to horizontality. The paleocurrent/azimuth data illustrated on the detailed profiles are plotted with respect to the outcrop orientation (cf. Miall, 1988a), as indicated on the left side of each profile (Figs 7, 10, 13 and 16). Note also the scale differences between each profile.

White Rock Mesa East (Fig. 7). The west half of this profile was previously documented by Miall and Turner-Peterson (1989, Fig. 15). The profile shown in Figure 7 of this paper contains paleoflow data from parting lineations not documented previously by Miall and Turner-Peterson (1989). Although the profile appears somewhat complex in terms of the number of subhorizontal third- and fifth-order surfaces that occur here, it is relatively simple when reduced down to intervals of coherent paleocurrent orientation, as indicated by the black arrows of cross-stratal dip directions (Xb) and parting lineation trends (Pl) (Fig. 7). Internally uniform paleocurrent intervals 1, 2 and 3, presented in Figure 8a and Table 2, correspond to sandstone units bounded by fifth-order bounding surfaces A-A', A'-A'', and A''-A''' respectively. The succeeding sandstone sheet is indicated by the fifth-order bounding surface B (surfaces not identified with primes represent laterally extensive fifth-order bounding surfaces, which are underlain by overbank fines, whereas surfaces with primes are laterally extensive fifth-order surfaces which are not underlain by overbank fines; third-order bounding surfaces comprise the remaining thick lines in the lateral profiles). The sandstone sheet represented by A to A''' most likely represents an amalgamated sandstone body, judging from the presence of locally preserved rafts of intraclasts along bounding surface A', and the fact that the paleocurrent trend of sandstone unit 1 between surfaces A and A' is highly divergent from the overlying sandstone units 2 and 3 (Fig. 8a). The high paleoflow dispersion was interpreted by Miall and Turner-Peterson (1989) to be the product of localized low-stage concentration of flow around erosional bar remnants. This may be the case for the middle sandstone unit 2, where orientations of parting lineations and corresponding cross-stratal dips differ (Fig. 8a), but the lower sandstone unit 1 can be interpreted as the result of channel flow at an angle to the rest of the fluvial system (at a much wider scale than the exposure). The top sandstone unit 3 is dominated by lithofacies Sh, Si and Sl, and displays highly random orientations of paleoflow structures from which the exact paleoflow direction cannot be determined (Fig. 8a, Table 2).

A striking aspect of this exposure is the presence of concave-up features which are bounded by discordant erosional basal third-order surfaces (BS3) (Fig. 9). There are several of these large structures in this profile, and they resemble "smaller channels" of Campbell (1976, his Fig. 5). These are commonly filled with lithofacies Si and Sl. The large concave-up "hollow" (*sensu* descriptive terminology of Friend 1983) marked 'V' (in Fig. 7) is symmetrically and vertically filled from both sides (Fig. 9). The longitudinal axial orientation of this particular structure trends 10°/250°. The lateral profile is, therefore, orientated oblique to the axial trend of this hollow. The significant axial dip of this structure indicates the non-horizontal and non-cylindrical nature of this hollow. Note that the axial dip azimuth of this hollow is obliquely upslope with respect to the paleoslope indicated by the surrounding paleoflow orientations (Fig. 9a, Table 2). The axial dip of one other hollow in this area indicated downstream dip with respect to the paleoflow, showing these hollows to be trough-like in three-dimensional geometry. However, plan exposures of these hollow structures are rare; thus, the three-dimensional aspect of this structure is poorly known. Unlike cosets of smaller trough cross-stratification, hollows commonly occur isolated from each other, but in some areas are grouped as described in the next section.

Kit Carson's Cave East (Fig. 10). This profile, located 0.5 km southeast of the east end of White Rock Mesa East profile, features horizons of overbank fines being truncated, and sandstone bodies becoming amalgamated to the south (i.e. to the right of profile). The lower horizon of overbank fines corresponds to the overbank fines located directly above sandstone unit 3 of White Rock Mesa East profile, and bounding surfaces A and B both correspond to bounding surfaces A and B of White Rock Mesa East profile (Fig. 7). The bounding surfaces marked with primes, however, are not likely the same surfaces as illustrated in the previous profile. The paleoflow is into the profile, enabling fairly good cross-sectional geometries to be determined from this exposure (Figs 8b, 10). Unfortunately most of the middle portion of this exposure is inaccessible, but it can be clearly seen from the profile that the dominant lithofacies is Si/Sl with some displaying parting lineations on their bedding surfaces. It can be appreciated from the profile that there is no meaningful cyclicity within the sandstone bodies in terms of their component lithofacies (Fig. 10).

As in the previous profile, the striking features are the large hollows, seen here in transverse view (Fig. 10). Detailed examination of the large-scale hollow on the central north end of the profile, labeled 'O', indicates lateral and oblique fill of the hollow with Si/Sl lithofacies exhibiting parting lineation on the bedding surfaces (Figs 11). The internal disposition of the stratified Si/Sl lithofacies can vary quite dramatically from one hollow to another; some being vertically filled (V), whereas others are laterally filled (L), or combinations of the above. In one case the lateral fill was composed of avalanche-face deposition, with angle-of-repose fine- to medium-grained sandstone (L; Fig 12). Hollows in the middle of the profile occur in a group, apparently along one horizon above a pebble clast-rich, laterally-continuous fifth-order bounding surface B', whereas other hollows are distinctly isolated. However, even when present in groups, the internal organization of the hollows and their scale is not uniform from one hollow to another (Fig. 10).

Shallow northerly dipping second- and third-order bounding surface traces can be identified between fifth-order bounding surfaces B and B', along the southern and central portion of the profile (LA). These dipping surfaces, which are bounded on the base by flat erosional surfaces, most likely represent sheet-like lateral-accretion elements, as described elsewhere from the Westwater Canyon Member by Miall and Turner-Peterson (1989). These features, however, contrast with the hollows, which are laterally restricted by concave-up third-order erosional bounding surfaces.

Kit Carson's Cave West (Fig. 13). The Kit Carson's Cave West profile is located 0.5 km southwest of Kit Carson's Cave East profile and their orientations are essentially the same (Fig. 4), but the Kit Carson's Cave West cliff exposure faces east. The paleoflow, therefore, is out of the profile, as indicated by the

Continued on page 86

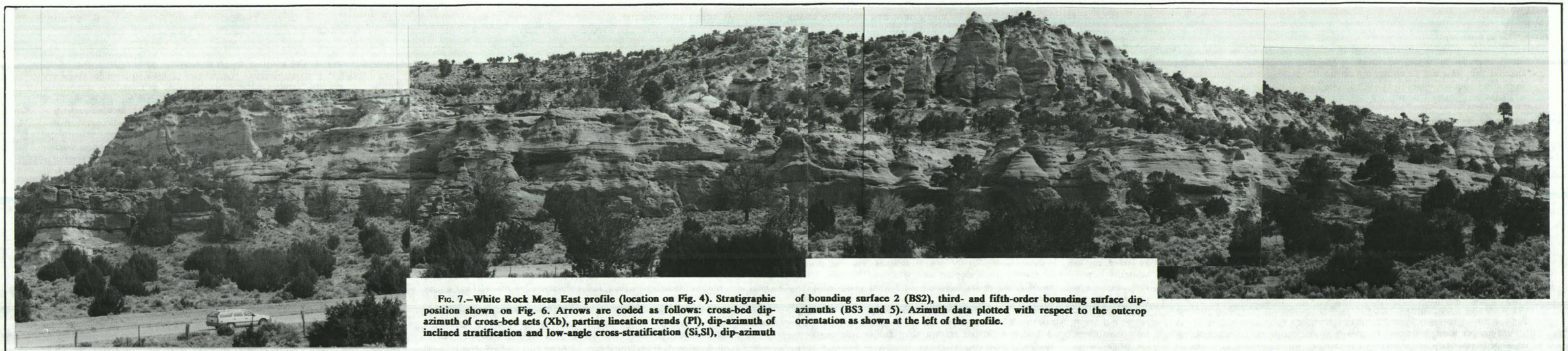

FIG. 7.–White Rock Mesa East profile (location on Fig. 4). Stratigraphic position shown on Fig. 6. Arrows are coded as follows: cross-bed dip-azimuth of cross-bed sets (Xb), parting lineation trends (Pl), dip-azimuth of inclined stratification and low-angle cross-stratification (Si,Sl), dip-azimuth of bounding surface 2 (BS2), third- and fifth-order bounding surface dip-azimuths (BS3 and 5). Azimuth data plotted with respect to the outcrop orientation as shown at the left of the profile.

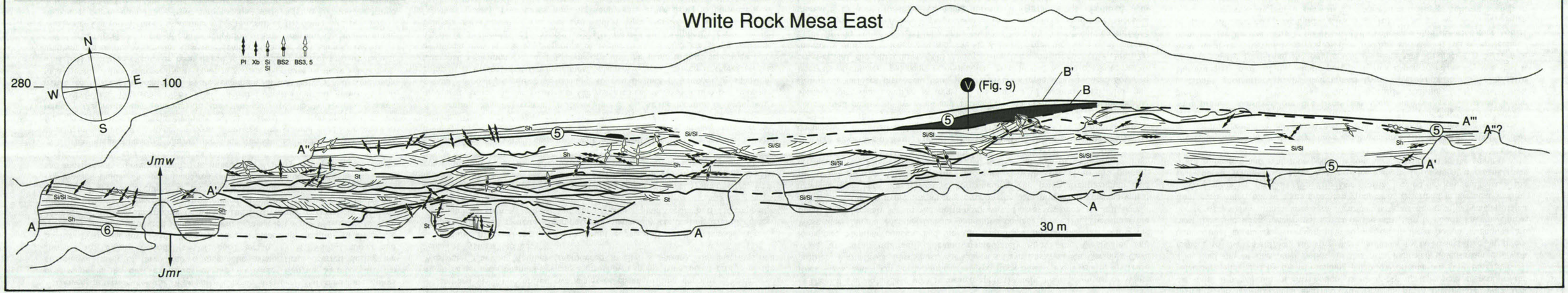

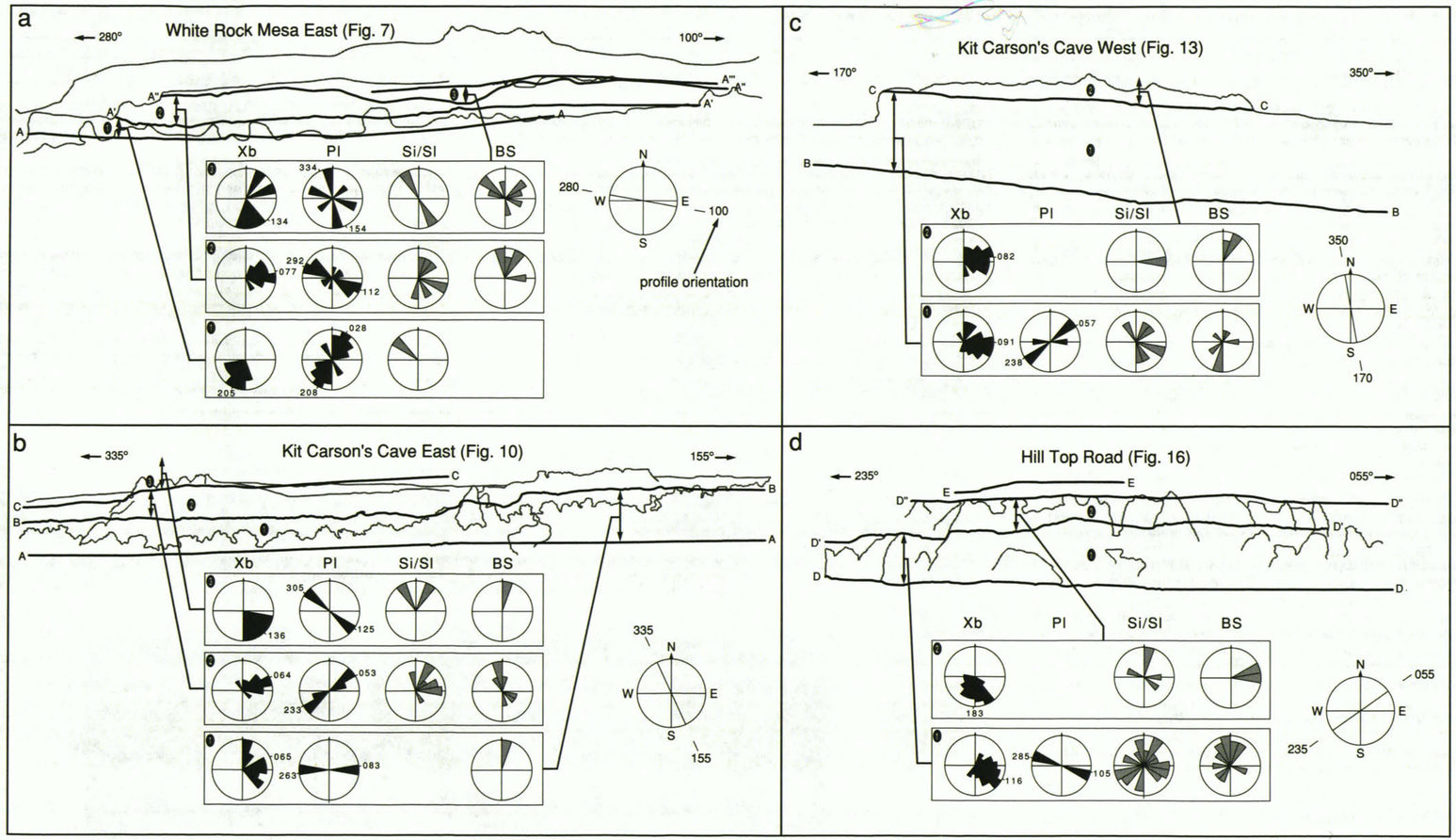

Fig. 8.—Paleocurrent, Si/Sl, and bounding surface orientation summary diagram for a. White Rock Mesa East; b. Kit Carson's Cave East; c. Kit Carson's Cave West; and d. Hill Top Road. The orientation data are subivided into coherent intervals separated by fifth-order bounding surfaces. Paleocurrent statistics are summarized in Table 2.

Table 2.--The paleocurrent and vector dip-azimuth statistics of the Kit Carson's Cave area profiles, as presented in Fig. 8. WRM East = White Rock Mesa East Profile; KCC East = Kit Carson's Cave East Profile; KCC West = Kit Carson's Cave Profile; HTR = Hill Top Road Profile. n = number of observations; V.M. = vector mean azimuth; σ = circular standard deviation; z = Raleigh's z test of random distribution (at the 5% significance level) where R, U, and B indicate random, nonrandom unidirectional and nonrandom bipolar distributions respectively. z test not conducted for sample numbers less than five.

		Xb				Pl				Si/Sl				BS			
		n	v.m.	σ	z	n	v.m.	σ	z	n	v.m.	σ	z	n	v.m.	σ	z
WRM East	1	7	205°	27°	U	9	208°	25°	B	2	316°	2°	-	15	077°	29°	U
	2	15	077°	29°	U	15	112°	26°	B	7	087°	74°	R	6	018°	32°	U
	3	5	134°	71°	R	6	154°	44°	R	2	241°	155°	-	10	004°	89°	R
KCC East	1	11	065°	46°	U	2	083°	3°	-					1	000°	-	-
	2	20	064°	31°	U	8	053°	9°	B	16	054°	40°	U	9	015°	72°	R
	3	4	136°	28°	-	1	125°	-	-	2	002°	29°	-	1	010°	-	-
KCC West	1	40	091°	47°	U	4	058°	15°	-	7	086°	67°	R	14	192°	78°	R
	2	16	082°	36°	U					1	095°	-	-	3	025°	8°	-
HTR	1	43	116°	41°	U	1	105°	-	-	31	059°	130°	R	14	341°	63°	U
	2	25	183°	35°	U					6	027°	70°	U	2	074°	8°	-

black arrows of cross-stratal dip directions (Xb) and parting lineation trends (Pl) (Fig. 13). In places, the outcrop is characterized by laterally extensive fifth-order bounding surfaces (A, B, B', C), whereas elsewhere it is dominated by discontinuous third-order bounding surfaces with locally very steep angular contacts (up to 26°). The laterally continuous bounding surfaces, with the exception of A, could not be demonstrated to be the equivalent of the surfaces of the previous two profiles, nor could paleocurrent trends within packages be correlated, illustrating the difficulty of correlating depositional packages from one exposure to another in this erosionally dissected terrain.

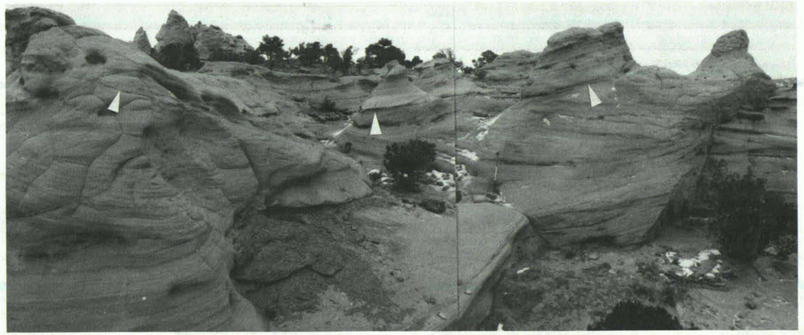

FIG. 9.—Vertically filled hollow (with Si) at White Rock Mesa East profile (see Fig. 7 for location). The axis of the structure dips ~10° toward the viewer, which is roughly up-paleoslope. The staff is 1.5 m long. Direction of view 070°.

The large inclined structure in the center of the profile (O) is an oblique view of another hollow, which is laterally/obliquely filled with lithofacies Si/Sl, with minor St and Sthb lithofacies (Fig. 14). The paleoflow is obliquely out and to the left in the lower sandstone unit 1 (Fig. 8c), and consistent with the axial trend of the hollow being slightly oblique to the exposure. The hollow and its fill resemble a lateral-accretion structure from this view (element LA of Miall, 1985), and similar structures were interpreted as such by Miall and Turner-Peterson (1989). On the other hand, its concave-up basal surface indicates it is a negative (erosional) feature, as opposed to the positive (constructional) feature of element LA normally developed on a laterally extensive flat erosional surface. A steep concave-up basal erosion surface also bounds the southern margin of another hollow marked 'V'. The discordant basal bounding surface dip of the hollow 'V' is 26° (Fig. 15), which is close to the maximum stable angle-of-repose for fine- to medium-grained sand.

In contrast to these laterally limited hollows, the structure labeled 'LA' may represent a lateral-accretion element (LA of Miall, 1985, 1988a, c). Its basal erosion surface is laterally extensive, and clearly flat, suggesting a lateral-accretion macroform developed on a laterally extensive flat erosional surface.

Hill Top Road (Fig. 16). The Hill Top Road profile, located 0.4 km east-northeast of White Rock Mesa East profile (Fig. 4), is the most detailed profile constructed in this area, and stratigraphically the highest profile from the Kit Carson's Cave area. The uppermost sheet sandstone present in the Kit Carson's Cave East profile (Fig. 10), bounded at the base by surface C, can be traced laterally to the base of Hill Top Road profile, where it is bounded on its top by surface D (Fig. 16). Most of the bounding surfaces, including first-order ones, can be seen in this profile, defining cross-stratified sets in the upper sandstone unit 2 (Figs 8d, 16). It can be seen that St in some places is gradational to lithofacies Si/Sl. The lower unit is characterized by abundant Si/Sl lithofacies, some of which appear as broad concave-up stratification. Isolated trough-shaped Sthb structures occur in the center and center left of the profile.

Upper sandstone unit 2, as represented by the unimodal orientation of sedimentary structures and uniform thickness, most likely represents a single channelbelt sandstone sheet, as described in part I of this paper. Bounding surface D' is most likely the base of a channelbelt sheet sandstone, judging from the abundance of intraclasts along this horizon. However, lateral exposures of this bounding surface do not reveal any preserved overbank fine deposits, which may have been lost due to extensive downcutting. The difference in paleocurrent orientations between sandstone units 1 and 2 (Fig. 8d) also support this interpretation, as the paleoflow in the lower sandstone unit 1 is out of the profile, whereas paleoflow in the upper unit is obliquely out to the left (Figs. 8d, 16). The sandstone interval D to D" here, therefore, most likely represents an amalgamated composite-sheet sandstone.

An inclined feature (O) is noticeable in the central portion of the profile, but its lateral extent to the right is not clear. Although its upper bounding surface appears locally convex-up, this is due to a perspective problem of an overhang. The structure seems to be localized and the concave-up nature of the lower third-order bounding surface can be better seen from the west, looking obliquely at the cliff face, suggesting an equivalence to the hollow structures seen elsewhere in the other profiles from this area. The structure is most likely skewed in orientation to the right (northeast) with respect to the underlying paleoflow indicators, and represents an oblique longitudinal section through a hollow. The other shallow structures, as expressed by the broad concave-up Si/Sl laminations in the lower sandstone unit 1, are most likely shallow versions of the concave-up hollows.

The lithofacies contacts present between bounding surfaces D' and D" are gently inclined to the left and may represent shallow laterally accreted surfaces similar to the dipping surfaces present in Kit Carson's Cave East profile as described above.

Interpretation of the internal sandstone-sheet architecture

Paleocurrent variability, as determined from a. the axes of trough cross-stratification, and b. parting lineation within the individual sandstone sheets, is remarkably consistent at any one location in the Kit Carson's Cave area (Fig. 8). This may indicate that the sandstone sheets record a single depositional/aggradational event. In some areas (e.g., White Rock Mesa East and Hill Top Road), it is difficult to determine if the fifth-order bounding surfaces are the expression of individual sheet-channel fills within a larger sheet-channelbelt sandstone body, or if they represent bases of amalgamated channelbelt sandstone deposits. In the absence of overbank fine deposits between the sandstone sheets, it was difficult to determine with certainty which is the case.

The origin of hollows described above can be interpreted in several ways. They may represent: 1. large-scale dune structures with only their toesets preserved; 2. elongate channels ("smaller channels" as speculated by Campbell, 1976, his Fig. 5,); or 3. some other type of scour-fill structure formed within the fluvial channel belt. The hollows were previously interpreted by Miall and Turner-Peterson (1989) to be ancient analogues of large elongate flute-like scours formed at channel bases, as documented by Coleman (1969) from the Brahmaputra River. The physical processes involved in the formation of these flute-like scours are not yet known. Similar, but smaller scale structures, have been documented from a ephemeral stream deposit by Olsen (1989), and interpreted to have been formed from the erosional action of spiral vortices developed during a sheet flooding event.

The internal organization of the hollow fills are somewhat variable from one hollow to another, and they can occur as isolated sets (Figs. 7, 10, 13, 16). These features do not resemble the regularity of large cross-bed sets reported from other fluvial sandstones such as the Hawkesbury Sandstone (cf. Conaghan and Jones, 1975), suggesting an origin other than that of dune preservation. Channels downcutting into sand banks, if formed, are not likely to be preserved with steep banks (in the order of 15° to 30°, as seen in the hollows of White Rock Mesa East and Kit Carson's Cave West profiles) due to the absence of fines and, therefore, lack of bank cohesion. Furthermore, the fact that the hollows are most likely trough-shaped in three dimensions suggests an origin other than elongated channelization.

A process for forming deep scours, of up to six times the mean channel depth, by channel convergence, has been documented both from rivers and from laboratory flumes (Mosley, 1976; Mosley and Schumm, 1976; Best and Brayshaw, 1985; Best 1987, 1988; Best and others, 1989). These studies suggest that a mechanism of deep scouring may be a significant process at channel junctions, and this is particularly the case for the sandy braided-stream environment, where stream junctions abound (cf. Best, 1987, p. 34; Best and others, 1989). Best (1987) for example has shown that avalanche faces can develop on the upstream end of these scours. This will allow the scours potentially to be filled laterally, obliquely or vertically by the avalanche deposit in a short period of time during channel switching or a flood event within a braided-fluvial setting. The scours are, therefore, envisaged to form as clusters or isolated features, depending on the density and spacing of the channels within a braided channelbelt.

Another mechanism of deep scouring in a braided fluvial environment was documented by Cant (1976) in the South Saskatchewan River. Cant (1976, p. 125) interpreted deep scours, reaching nearly three times the mean braid-channel depth, to have formed upstream of a large emergent bar. This process is analogous to scouring on the upstream margin of an obstacle clast in a flow (cf. Best and Brayshaw, 1985), with the emergent bar acting as an obstacle within the channel. This scour-and-fill process may also be a significant process governing the final depositional state of multichannel braided fluvial systems, in addition to the above mentioned scour process, which occurs at channel confluences. The laterally restricted hollows erode underlying material, which in some places appears to be composed of inclined lateral-accretion macroforms (Kit Carlson's Cave East profile, Fig. 10). The hollows may represent initial stages in the development of laterally extensive macroforms, since their internal-stratification geometries appear similar.

DISCUSSION

Typical fluvial-sandstone body dimensions

Friend (1983) classified channels into three types: fixed, meandering, and braided, which result in two different types of sandstone-body morphology. Channels that are stable between avulsive events commonly create ribbon bodies, whereas channels that steadily migrate laterally within a channelbelt will create sheet-like sandbodies, whether they are meandering or braided (Friend 1983).

The sheet sandstones, which represent channelbelt deposits that have aggraded between avulsive events, can form thicker amalgamated sandstone bodies if the subsidence between avulsive events is not fast enough to allow preservation of intervening overbank fines. The field distinction between individual sheet sandstone bodies (cf. Friend, 1983, p. 350) can only be made from interpretation of large, laterally continuous exposures orientated transverse to the paleoflow direction. At present there are a few documented examples indicating what range of thicknesses and widths individual sheet bodies can attain. Commonly, when figures are given, the authors do not specify which of the following four possible cases these dimensions represent: 1. dimensions of the channel-fill sandstones and fines within a larger channelbelt deposit; 2. dimensions of the channelbelt deposit; 3. dimensions of an amalgamated channelbelt deposit (i.e. composite sandstone bodies); or 4. some combination of the above cases. However, following the suggestions of Collinson (1978) and Friend and others (1979), reports of the cross-sectional dimensions of fluvial sandstone body dimensions have increased in the last decade, allowing a review of the expected ranges of channelbelt sandstone body dimensions resulting from fluvial deposition. Published ranges of widths and thicknesses of sandstone bodies and their interpreted fluvial styles are summarized in Figure 17.

The data presented in Figure 17 can broadly be divided into three classes: sandbody dimensions that are divided into 1. ribbons and 2. sheets following the suggestion of Friend and others (1979) and shown as circles and squares, respectively, in Fig. 17, and 3. some thicker sandstone-sheet deposits that are

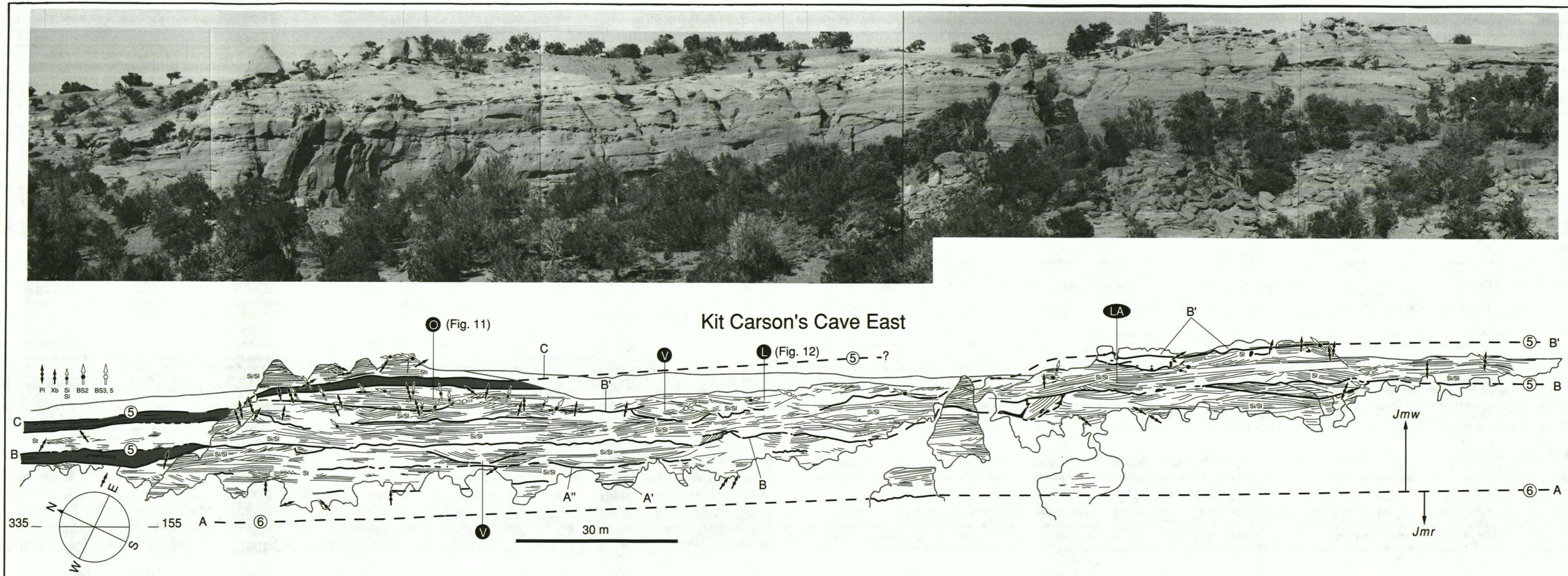

Fig. 10.—Kit Carson's Cave East profile (location on Fig. 4). Stratigraphic position shown on Fig. 6. Azimuth data same scheme as Fig. 7.

FIG. 11.—Southern erosional margin and fill of the hollow labeled "O" in Kit Carson's Cave East profile (see Fig. 10). The azimuth data (as indicated) show that the internal fill of lithofacies Sl is filled obliquely with respect to the strike of the hollow base. Direction of view 350°.

FIG. 12.—Direction of view 085° along strike of the south end of a hollow labeled "L" at Kit Carson's Cave East profile (see Fig. 10). The hollow is laterally filled by two cross-stratified sets. The 1.5 m scale on top is parallel to the plan trace of the cross-strata.

composite in nature (amalgamated sheets), as far as can be gathered from the documentation. This third class plots in the upper right of the diagram (shown as diamonds in Fig. 17). The single-sheet bodies, interpreted to be of channel/channelbelt origin, display wide ranges of sandstone widths, but they consistently show thicknesses less than 12 m. In general, the inferred braided deposits have a wider range of thicknesses than meandering deposits, but the reported sandstone-body dimensions cluster between 1 and 12 m in thickness. These figures, which are independent of fluvial style or tectonic setting, suggest that regardless of the original channel depth, erosion or some other processes result in the preservation of fairly consistent thicknesses of 1-12 m. It is worth noting that although thickness of sandstone sheets can easily be deciphered in the field, less confidence can be placed on actual widths of sandstone sheets, even in areas of wide exposure such as the Westwater Canyon Member, due to their very high width:thickness ratios. The range of channelbelt sandstone widths as plotted on Figure 17, therefore, most likely includes laterally amalgamated widths.

Exceptions to the channelbelt thicknesses of 1-12 m are those of non-channelized sheet-flood deposits (Olsen, 1989; Tunbridge, 1981), which display very low thickness values of less than 1 m (18 and 31 in Fig. 17). One very thick point-bar channelbelt deposit (Mossop and Flach, 1983), and various fixed channels (Hopkins, 1985), both from the Alberta Foreland Basin, record preservation of very deep channel deposits in tidal to deltaic distributary settings, respectively (30 and 37 in Fig. 17). Hopkins (1985, p. 49) suggested that deep channel incision is independent of base level changes in deltaic settings, pointing out that channelization of up to 60 m below sea level is reported from a modern delta distributary (Meckel, 1972). Further studies of fluvial sandbody geometries may reveal other deep-river channelbelt bodies and shed light on the controls of deep river deposition and preservation.

Dimensions of the Westwater Canyon Member sandstone bodies

The ~5- 10-m-thick sheet-sandstone bodies of the Westwater Canyon Member represent channelbelt deposits that aggraded between avulsive events (Fig. 18). The consistent paleocurrent trends within a sheet sandstone deposit suggest that a single depositional event created each sheet-sandstone body. The estimated sandstone-body thicknesses of the Westwater Canyon Member are well within the range of the clustered values (shown as 'w' in Fig. 17). In contrast, the sandstone thicknesses as reported by Campbell (1976) are within the range of amalgamated or composite sandstone bodies (shown as 'W' in Fig. 17). The wide range of "channel-system" dimensions as documented by Campbell (1976) is expected if amalgamation of more regular channelbelt deposits occurs at random (cf. Bridge and Leeder, 1979, see their Figs. 2c and 4c).

Cliff exposures of the Westwater Canyon Member serve as an excellent example for illustrating the control of overbank fines as effective barriers to pore-fluid flow. It is apparent that on the member scale, the preservation of overbank-fine deposits between sheet-like sandstone bodies has controlled the pore-fluid flow, notwithstanding the internal complexity of the sheet-sandstone architecture as revealed by the detailed lateral profiles. The sheet sandstones, with very little internal grain-size variation, acted as fluid conduits, and the thicknesses of conduits or compartments were solely dependent upon the preservation of overbank fines between the interpreted channelbelt sandstone bodies. The review of published examples of fluvial-body dimensions indicates a consistency of sandbody thicknesses, namely in the 1- to 12-m range, and the thicknesses of the Westwater sheets fit in this range (Fig. 17). The pore-fluid flow, therefore, will be largely confined within this thickness for sandy fluvial systems. Increases in this thickness range will be the result of amalgamation of the unit sandstone sheets by erosion of capping overbank fines, whereas a decrease is likely to be associated with increasing heterogeneity of grain size within the sandstone channelbelt bodies (as in deposits resulting from mixed-load fluvial systems).

Implications of hollow preservation

Fluvial sedimentologists have concentrated on the sedimentary features formed from the migration of positive barforms, and used these structures to decipher styles of fluvial sedimentation (Allen, 1983b; Haszeldine, 1983; Miall, 1988a). Little attention has been directed to processes in the deepest portions of fluvial channels until only recently (e.g., Best and others, 1989). Theoretically, it is not considered possible to preserve the entire thickness of the channelbelt deposit, and entire macroforms, unless avulsion of the channel belt takes place (cf. Bridge and Leeder, 1979). However, scour-fill processes, as documented by workers such as Best (1987) and Cant (1976), are comparatively more ephemeral, in a multichannel fluvial system, than life of constructional macroforms; it is likely that these structures with high preservation potential deposited in the deepest parts of the channel belts may dominate the geological record. The abundant hollows as seen in the Westwater Canyon Member may represent such scours from the deepest portions of the channel belt.

CONCLUSIONS

Several significant conclusions can be drawn from this study of the large-scale features of the Westwater Canyon Member.

1. The "channel systems" described by Campbell (1976, Fig. 3 herein) are not channelbelt deposits but records of post-depositional pore-water conduits composed of amalgamated, ~5- 10-m-thick sheet sandstone bodies.

2. The individual sheet-sandstone-body thickness of the Westwater Canyon Member falls within the thickness ranges of sandstone bodies that are of possible channelbelt origin. Sandstone body thicknesses in excess of 12 m appear to result from channelbelt amalgamation.

3. Diagenetic pore-fluid flow was primarily controlled by the presence of thick overbank deposits which escaped erosion during amalgamation of channelbelt sandstone bodies. Published data on fluvial deposits indicate that large-scale pore-fluid conduits composed of homogeneous channelbelt sandbodies fall within the 1-12 m thickness range. Departures from this range are expected to be due either to channelbelt amalgamation or higher heterogeneity within the sandstone sheet.

4. Internally, sheets display trough-like features ~30 x 5 m in cross-section dimensions, commonly isolated, with varying orientations of internal fill. The interpretation of these large-scale hollow features is most consistent with a scour produced within the deepest portions of a shallow, braided-fluvial environment, possibly due to channel-confluence scouring. The variable inclination of the fills, with parting lineation on their bedding surfaces, are most consistent with a rapidly filled scour and are less consistent with forms produced from trains of large dunes or small channels, as previously interpreted.

5. The member contains low-amplitude, laterally extensive macroforms bounded by flat erosional surfaces, consistent with the interpretation that the style of the fluvial environment was a braided multichannel system. Hollows, on the other hand, are bounded by concave-up erosional surfaces and are interpreted to have been produced in the deepest portions of the fluvial channel belt, and hence have greater preservation potential than constructional macroforms.

ACKNOWLEDGMENTS

This work was completed while the author was the recipient of a Canadian Commonwealth Scholarship. Acknowledgment is made to the donors of the American Chemical Society Petroleum Research Fund, AAPG Grants in Aid, and to NSERC for support of this project through research grants to my supervisor A.D. Miall. I thank the Navajo Nation (Window Rock, AZ) for allowing field work to be conducted on the Navajo Indian Reservation. I am indebted both to Andrew Miall who initially suggested reexamining the large-scale architecture of the Westwater Canyon Member, and to Christine E. Turner-Peterson whose guidance in and out of the field was most appreciated. Andrew D. Miall, Greg C. Nadon, Alan C. Kendall, Nick Eyles and Paul D. Godin (who also assisted in the field) are thanked for stimulating discussion and comments on the manuscript during various stages of the study. Constructive criticism by reviewers C. E. Turner-Peterson and A. Ramos served to greatly improve the manuscript. The oblique aerial photographs used to construct Figures 5 and 6 were photographed by A.D. Miall and reproduced by Brian O'Donovan.

REFERENCES

ALEXANDER, J., AND LEEDER, M. R., 1987, Active tectonic control on alluvial architecture, *in* Ethridge, F. G., Flores, R. M., and Harvey, M. D., eds, Recent developments in fluvial sedimentology: Society of Economic Paleontologists and Mineralogists Special Publication 39, p. 243-252.

ALLEN, J. R. L., 1978, Studies in fluviatile sedimentation: An exploratory quantitative model for the architecture of avulsion-controlled alluvial suites: Sedimentary Geology, v. 21, p. 129-147.

_____, 1983a, Gravel overpassing on humpback bars with mixed sediment: examples from the Lower Old Red Sandstone, southern Britain: Sedimentology, v. 30, p. 285-294.

_____, 1983b, Studies in fluviatile sedimentation : bars, bar-complexes and sandstone sheets (low-sinuosity braided streams) in the Brownstones (L. Devonian), Welsh Borders: Sedimentary Geology, v. 33, p. 237-293.

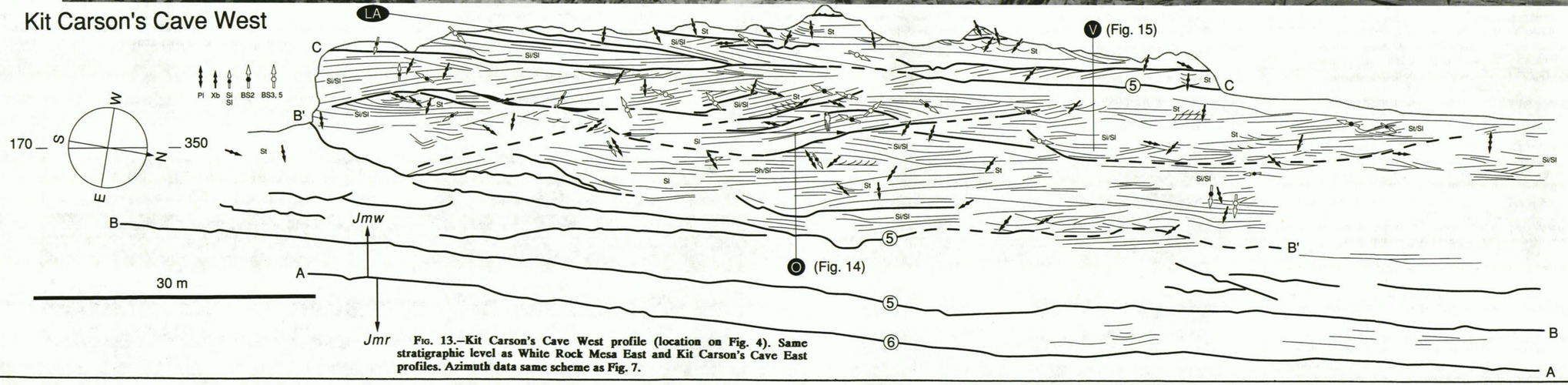

FIG. 13.—Kit Carson's Cave West profile (location on Fig. 4). Same stratigraphic level as White Rock Mesa East and Kit Carson's Cave East profiles. Azimuth data same scheme as Fig. 7.

Fig. 14.—A closeup view of the northern end of the large hollow labeled "O" at Kit Carson's Cave West profile (see Fig. 13). The discordant third-order bounding surface is marked by arrows. The fill is mainly lithofacies Si and Sl. Direction of view 260°.

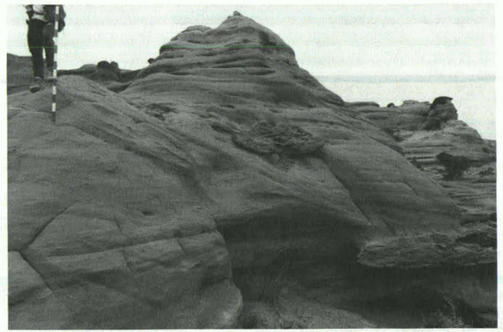

Fig. 15.—The southern erosional margin of the hollow labeled "V" at Kit Carson's Cave West profile (see Fig. 13). The dip of the basal margin and overlying attitude of lithofacies Si is 26°. The staff with 10 cm markings rest on the basal surface trace. Direction of view 260°.

Beer, J. A., and Jordan, T. E., 1989, The effects of Neogene thrusting on deposition in the Bermejo Basin, Argentina: Journal of Sedimentary Petrology, v. 59, p. 330-345.

Behrensmeyer, A. K., and Tauxe, L., 1982, Isochronous fluvial systems in Miocene deposits of Northern Pakistan: Sedimentology, v. 29, p. 331-352.

Best, J. L., 1987, Flow dynamics at river channel confluences: implications for sediment transport and bed morphology, *in* Ethridge, F. G., and Flores, R. M., eds, Recent and ancient nonmarine depositional environments, Society of Economic Paleontologists and Mineralogists Special Publication 31, p. 27-35.

_____, 1988, Sediment transport and bed morphology at river channel confluences: Sedimentology, v. 35, p. 481-498.

_____, and Brayshaw, A. C., 1985, Flow separation - a physical process for the concentration of heavy minerals within alluvial channels: Journal of the Geological Society, London, v. 142, p. 747-755.

_____, Bristow, C. S., and Roy, A. G., 1989, The morphology of river channel confluences: scales and dynamics, Program and Abstracts of the 4th International Conference on Fluvial Sedimentology, Barcelona, Sitges, p. 75.

Blakey, R. C., and Gubitosa, R., 1984, Controls of sandstone body geometry and architecture in the Chinle Formation (Upper Triassic), Colorado Plateau: Sedimentary Geology, v. 38, p. 51-86.

Bridge, J. S., and Leeder, M. R., 1979, A simulation model of alluvial stratigraphy: Sedimentology, v. 26, p. 617-644.

Campbell, C. V., 1976, Reservoir geometry of a fluvial sheet sandstone: American Association of Petroleum Geologists Bulletin, v. 60, p. 1009-1020.

Cant, D. J., 1976, Braided stream sedimentation in the South Saskatchewan River: unpublished Ph.D. thesis, McMaster University, Hamilton.

_____, 1978, Fluvial facies models and their application, *in* Scholle, P. A., and Spearing, D., eds, Sandstone depositional environments, American Association of Petroleum Geologists Memoir 31, p. 115-137.

Coleman, J. M., 1969, Brahmaputra River: channel processes and sedimentation: Sedimentary Geology, v. 3, p. 129-239.

Collinson, J. D., 1978, Vertical sequence and sand body shape in alluvial sequences, *in* Miall, A. D., ed., Fluvial sedimentology, Canadian Society of Petroleum Geologists Memoir 5, p. 577-586.

_____, 1986, Alluvial Sediments, *in* Reading, H. G., Sedimentary environments and facies: Blackwell Scientific Publications, p. 20-62.

Conaghan, P. J., and Jones, J. G., 1975, The Hawkesbury Sandstone and the Brahmaputra: a depositional model for continental sheet sandstones: Journal of the Geological Society of Australia, v. 22, p. 275-283.

Cowan, E. J., 1990, The fluvial sedimentology of the Westwater Canyon Member, Morrison Formation (Jurassic), San Juan Basin, New Mexico, USA: unpublished M.Sc. thesis, University of Toronto, 162 p.

Friend, P. F., 1983, Towards the field classification of alluvial architecture or sequence, *in* Collinson, J. D., and Lewin, J., eds, Modern and ancient fluvial systems: International Association of Sedimentologists Special Publication 6, p. 345-354.

_____, Slater, M. J., and Williams, R. C., 1979, Vertical and lateral building of river sandstone bodies, Ebro Basin, Spain: Journal of the Geolical Society, London, v. 136, p. 39-46.

Galloway, W. E., 1981, Depositional architecture of Cenozoic gulf coastal plain fluvial systems, *in* Ethridge, F. G., and Flores, M. R., eds, Recent and ancient nonmarine depositional environments: models for exploration: Society of Economic Paleontologists and Mineralogists Special Publication 31, p. 127-155.

Gibling, M. R., and Rust, B. R., 1990, Ribbon sandstones in the Pennsylvanian Waddens Cove Formation, Sydney Basin, Atlantic Canada: the influence of siliceous duricrusts on channel-body geometry: Sedimentology, v. 37, p. 45-65.

Godin, P. D., 1991, Fining-upward cycles in the sandy braided-river deposits of the Westwater Canyon Member (Upper Jurassic), Morrison Formation, New Mexico: Sedimentary Geology, v. 70, p. 61-82.

Granger, H. C., and Santos, E. S., 1986, Geology and ore deposits of the Section 23 mine, Ambrosia Lake District, New Mexico, *in* Turner-Peterson, C. E., Santos, E. S., and Fishman, N. S., eds, A basin analysis case study: Morrison Formation Grants Uranium Region New Mexico, American Association of Petroleum Geologists Studies in Geology 22, p. 185-210.

Hackman, R. J., and Olsen, A. B., 1977, Geology, structure and uranium deposits of the 1x2° quadrangle, New Mexico and Arizona, U.S. Geological Survey Miscellaneous Investigations Series I-981, scale 1:250,000.

Hansley, P. L., 1986, Regional diagenetic trends and uranium mineralization in the Morrison Formation across the Grants Uranium Region, *in* Turner-Peterson, C. E., Santos, E. S., and Fishman, N. S., eds, A basin analysis case study: The Morrison Formation Grants Uranium Region New Mexico, American Association of Petroleum Geologists Studies in Geology 22, p. 277-301.

Haszeldine, R. S., 1983, Fluvial bars reconstructed from a deep, straight channel, Upper Carboniferous coalfield of northeast England: Journal of Sedimentary Petrology, v. 53, p. 1233-1247.

Hopkins, J. C., 1985, Channel-fill deposits formed by aggradation in deeply scoured, superimposed distributaries of the Lower Kootenai Formation (Cretaceous): Journal of Sedimentary Petrology, v. 55, p. 42-52.

Kraus, M. J., and Middleton, L. T., 1987, Contrasting architecture of two alluvial suites in different structural settings, *in* Ethridge, F. G., Flores, R. M., and Harvey, M. D., eds, Recent developments in fluvial sedimentology: Society of Economic Paleontologists and Mineralogists Special Publication 39, p. 253-262.

Lawrence, D. A., and Williams, B. P. J., 1987, Evolution of drainage systems in responce to Acadian deformation: The Devonian Battery Point Formation, eastern Canada, *in* Ethridge, F. G., Flores, R. M., and Harvey, M. D., eds, Recent developments in fluvial sedimentology: Society of Economic Paleontologists and Mineralogists Special Publication 39, p. 263-300.

Leeder, M. R., 1978, A quantitative stratigraphic model of alluvium with special reference to channel deposit density and interconnectedness, *in* Miall, A. D., ed., Fluvial sedimentology: Canadian Society of Petroleum Geologists Memoir 5, p. 587-596.

_____, 1982, Sedimentology: London, George Allen and Unwin, 343 p.

Marzo, M., Nijman, W., and Puigdefabregas, C., 1988, Architecture of the Castissent fluvial sheet sandstones, Eocene, South Pyrenees, Spain: Sedimentology, v. 35, p. 719-738.

Meckel, L. D., 1972, Anatomy of distributary channel-fill deposits in Recent mud deltas (Abstract): American Association of Petroleum Geologists Bulletin, v. 56, p. 639.

Miall, A. D., 1978, Lithofacies and vertical profile models in braided river deposits: a summary, *in* Miall, A. D., ed., Fluvial sedimentology, Canadian Society of Petroleum Geologists Memoir 5, p. 597-604.

_____, 1985, Architectural-Element Analysis: a new method of facies analysis applied to fluvial deposits: Earth Sciience Reviews, v. 22, p. 261-308.

_____, 1988a, Architectural elements and bounding surfaces in fluvial deposits: Anatomy of the Kayenta Formation (Lower Jurassic), southwest Colorado: Sedimentary Geology, v. 55, p. 233-262.

_____, 1988b, Reservoir heterogeneities in fluvial sandstones: lessons from outcrop studies: American Association of Petroleum Geologists Bulletin, v. 72, p. 682-697.

_____, 1988c, Facies architecture in clastic sedimentary basins, *in* Kleinspehn, K. L., and Paola, C., eds, New Perspectives in basin analysis: New York, Springer-Verlag, p. 67-81.

_____, and Turner-Peterson, C. E., 1989, Variations in fluvial style in the Westwater Canyon Member, Morrison Formation (Jurassic), San Juan Basin, Colorado Plateau: Sedimentary Geology, v. 63, p. 21-60.

Mosley, M. P., 1976, An experimental study of channel confluences: Journal of Geology, v. 84, p. 535-562.

_____, and Schumm, S. A., 1976, Stream junctions - a probable locations for bedrock placers: Economic Geology, v. 72, p. 691-697.

Mossop, G. D., and Flach, P. D., 1983, Deep channel sedimentation in the Lower Cretaceous McMurray Formation, Athabasca Oil Sands, Alberta: Sedimentology, v. 30, p. 493-509.

Nami, M., and Leeder, M. R., 1978, Changing channel morphology and magnitude in the Scalby Formation (M. Jurassic) of Yorkshire, England, *in* Miall, A. D., ed., Fluvial sedimentology: Canadian Society of Petroleum Geologists Memoir 5, p. 431-440.

Olsen, H., 1989, Sandstone-body structures and ephemeral stream processes in the Dinosuar Canyon Member, Moenave Formation (Lower Jurassic), Utah, U.S.A.: Sedimentary Geology, v. 61, p. 207-221.

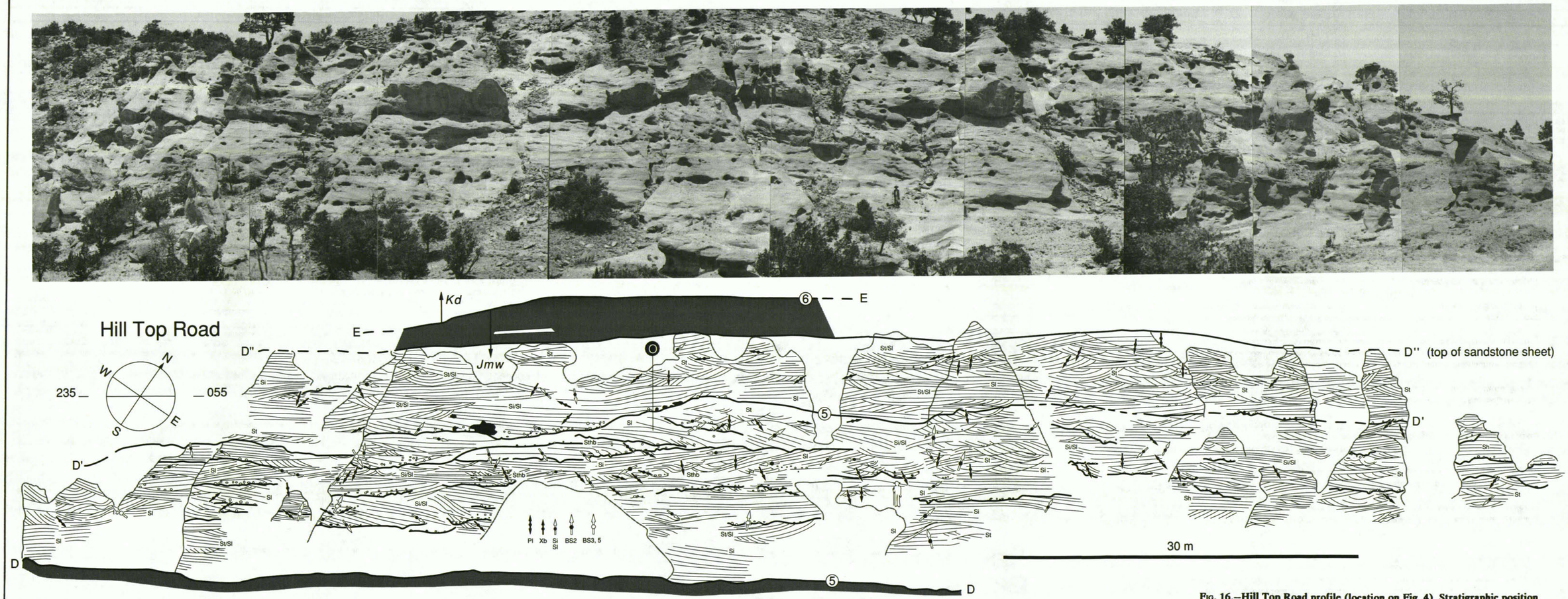

FIG. 16.—Hill Top Road profile (location on Fig. 4). Stratigraphic position shown on Fig. 6. Azimuth data same scheme as Fig. 7.

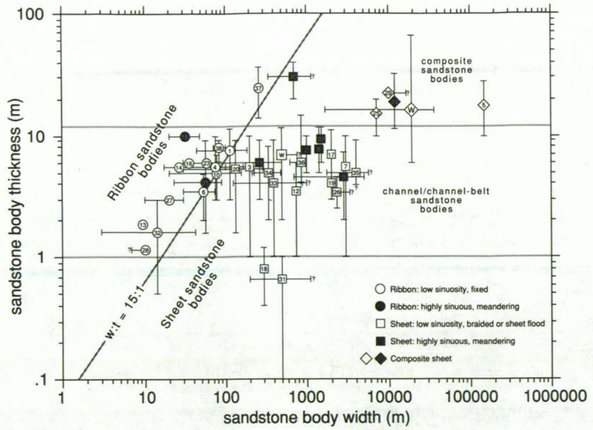

FIG. 17.—Log/log plot of published width:thickness dimensions of sandstone bodies, with ranges indicated by the bars. Published data which did not indicate ranges are not plotted with bars. Sources as follows: 1 and 2, Abrahamkraal Fm., Stear (1980); 3-6, Chinle Fm., Blakey and Gubitosa (1984), width ranges of 4 and 6 estimated assuming width:thickness ratio of 15:1; 7 and 8, Castissent Fm., Marzo and others (1988); 9, Middle Siwalik, Behrensmeyer and Tauxe (1982); 10 and 11, Scalby Fm., Nami and Leeder (1978); 12, Ft Prevel Fm., Lawrence and Williams (1987); 13 - 16, Oligocene and Miocene of Ebro Basin, Friend and others (1979); 17 - 19, Brownstones, Tunbridge (1981); 20 and 21, Salt Wash Member, Morrison Fm., Peterson (1984), width ranges of 22 estimated assuming width:thickness ratio of 15:1; 22 - 24, Willwood Fm., Kraus and Middleton (1987); 25, George West Axis, Oakville Fm., Galloway (1981); 26 and 28, Archer City and Nocona Fms., Sander (1989); 29, Beaufort Fm., Turner and Whately (1983); 30, McMurray Fm., Mossop and Flach (1983); 31, 32 and 33, sheet, simple and multistorey sandbodies respectively, Dinosaur Canyon Mbr, Mocnave Fm., Olsen (1989); 34, 35 and 36, Jarillal, Huachipampa and Quebrada del Cura Fms., Beer and Jordan (1989); 37, Lower Kootenai Fm., Hopkins (1985); 38, Waddens Cove Fm., Gibling and Rust (1990); W, "channel system" dimensions of the Westwater Canyon Member as given by Campbell (1976); w, estimated sheet sandstone body dimensions of the Westwater Canyon Member as presented herein, minimum width only, maximum not known.

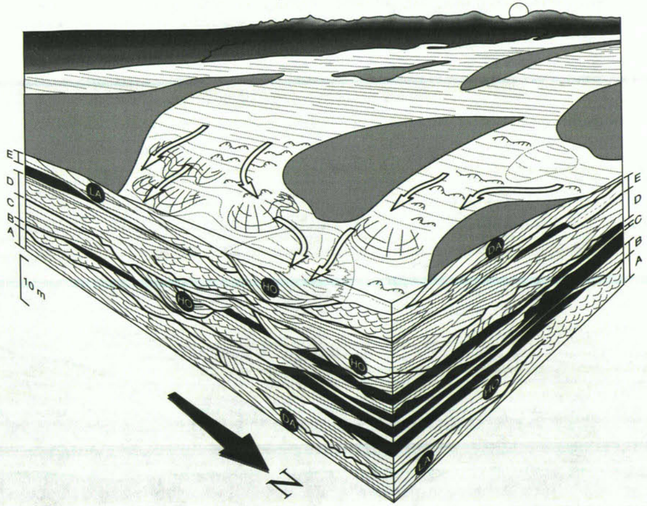

FIG. 18.—The large-scale architectural model of the Westwater Canyon Member fluvial system. The block diagram illustrates waning-stage flow, seen looking toward the southwest and the Late Jurassic magmatic arc. The sandstone units produced between each avulsive event of the channel belt are approximately 5 m thick, and are bounded by laterally-extensive fifth-order bounding surfaces. The width of the sandstone sheets is most likely >1 km. The sandstone bodies can be either single or composite channelbelt sandstones, depending on their vertical stacking, as shown by the examples of sandstone sheets A to E. The large hollows (labelled HO) within the sandstone sheets are interpreted as channel-confluence scours produced downstream of emergent channel sand bars, which in turn produce low-amplitude lateral accretion (LA) and downstream accretion (DA) deposits.

PAOLA, C., WIELE, S. W., AND REINHART, M. A., 1989, Upper-regime parallel lamination as the result of turbulent transport and low-amplitude bedforms: Sedimentology, v. 36, p. 47-59.

PETERSON, F., 1984, Fluvial sedimentation on a quivering craton: Influence of slight crustal movements on fluvial processes, Upper Jurassic Morrison Formation, western Colorado Plateau: Sedimentary Geology, v. 38, p. 21-50.

SANDER, P. M., 1989, Early Permian depositional environments and pond bonebeds in central Archer County, Texas: Palaeogeography, Palaeoclimatology, Palaeoecology, v. 69, p. 1-21.

SANTOS, E. S., AND TURNER-PETERSON, C. E., 1986, Tectonic setting of the San Juan Basin in the Jurassic, *in* Turner-Peterson, C. E., Santos, E. S., and Fishman, N. S., eds, A basin analysis case study: Morrison Formation Grants Uranium Region New Mexico, American Association of Petroleum Geologists Studies in Geology 22, p. 27-33.

SANDERSON, H. C., AND LOCKETT, F. P. J., 1983, Flume experiments on bedforms and structures at the dune-plane bed transition, *in* Collinson, J. D., and Lewin, J., eds, Modern and ancient fluvial systems: International Association of Sedimentologists Special Publication 6, p. 49-58.

STEAR, W. M., 1980, Channel sandstone and bar morphology of the Beaufort Group uranium district near Beaufort West: Transactions of the Geological Society of South Africa, v. 83, p. 391-398.

TUNBRIDGE, I. P., 1981, Old Red Sandstone Sedimentation - An example from the Brownstones (highest Lower Old Red Sandstone) of South Central Wales: Geological Journal, v. 16, p. 111-124.

TURNER, B. R., AND WHATELEY, M. K. G., 1983, Structural and sedimentation controls of coal deposition in the Nongoma graben, northern Zululand, South Africa, *in* Collinson, J. D., and Lewin, J., eds, Modern and ancient fluvial systems, International Association of Sedimentologists Special Publication 6, p. 457-471.

TURNER-PETERSON, C. E., 1985, Lacustrine-humate model for primary uranium ore deposits, Grants uranium region, New Mexico: American Association of Petroleum Geologists Bulletin, v. 69, p. 1999-2020.

_____, 1986, Fluvial sedimentology of a major uranium-bearing sandstone - a study of the Westwater Canyon Member of the Morrison Formation, San Juan Basin, New Mexico, *in* Turner-Peterson, C. E., Santos, E. S., and Fishman, N. S., eds, A basin analysis case study: Morrison Formation Grants Uranium Region New Mexico: American Association of Petroleum Geologists Studies in Geology 22, p. 47-75.

_____, AND FISHMAN, N. S., 1986, Geologic synthesis and genetic models fro uranium mineralization in the Morrison Formation, Grants uranium region, New Mexico, *in* Turner-Peterson, C. E., Santos, E. S., and Fishman, N. S., eds, A Basin Analysis Case Study: Morrison Formation Grants Uranium Region New Mexico: American Association of Petroleum Geologists Studies in Geology 22, p. 357-388.

_____, AND _____, 1988, Origin and distribution of albite, illite/smectite, and chlorite in Jurassic Lake T'oo'dichi': consequence of early diagenesis in saline, alkaline lake: Geological Society of America Abstracts with Program, v. 20, p. A51-52.